Structure of Ni-B-Melts by Means of X-Ray Diffraction

E. Nassif*, P. Lamparter, B. Sedelmeyer, and S. Steeb

Max-Planck-Institut für Metallforschung, Institut für Werkstoffwissenschaften, Stuttgart

Z. Naturforsch. **38a**, 1098–1102 (1983); received June 16, 1983

The structural results for molten $Ni_{81}B_{19}$ are compared with the structure of a metallic glass which can be obtained at the same composition by rapid quenching the melt within a melt spin equipment. Structural relationship exists between the molten and the amorphous state. This feature follows especially from a marked asymmetry of the second maximum of the structure factor obtained from the melts, to which corresponds the splitting up of the second maximum in the total structure factor of the amorphous specimen. With the $Ni_{53}B_{47}$- and the $Ni_{43}B_{57}$-melts which don't belong to the concentration range of glass-forming Ni-B-melts no peculiarities in the range of the second maximum of the structure factor were observed.

Introduction

Recently the three partial structure factors for amorphous $Ni_{81}B_{19}$ could be evaluated [1] and with the present paper the structural relationship between this amorphous phase and the corresponding melt shall be studied. In order to find out a correlation between the structure factor of the melt and its glass forming ability, and to study structural changes with increasing boron concentration, two further melts shall be studied which do not belong to the concentration region in which glass forming Ni-B-melts exist. This region reaches according to [2] up to 43 at.% B using the melt spin technique.

Concerning the theoretical fundamentals we refer to [3].

Experimental

The experimental facts are the same as reported in [3] with the following exceptions: The diffraction experiments using Mo-Kα-radiation were done in the high temperature chamber of a $\theta-\theta$ diffractometer under high vacuum of about 10^{-5} mbar. The step width was varied between 0.25 and 0.6° in 2θ. The resolution amounted to $\Delta 2\theta = 0.35°$ at the main peak.

Results and Discussion

I. Molten Ni-B- Containing 19 at.% B

a) Structure Factor

In Fig. 1 the Ashcroft-Langreth structure factor of the $Ni_{81}B_{19}$-melt is compared with the structure factors obtained from amorphous $Ni_{81}B_{19}$ [4], from molten $Fe_{83}B_{17}$ [5], and from amorphous $Fe_{80}B_{20}$ [5].

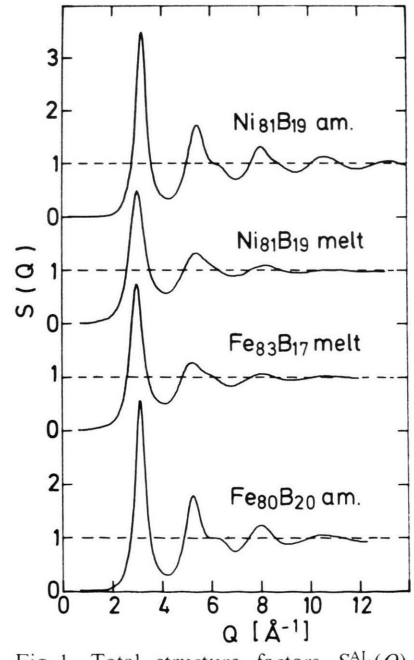

Fig. 1. Total structure factors $S^{AL}(Q)$ measured using Mo-Kα-radiation for amorphous $Ni_{81}B_{19}$ [4], molten $Ni_{81}B_{19}$, molten $Fe_{83}B_{17}$ [5], and amorphous $Fe_{80}B_{20}$ [5].

* On leave of Departamento de Fisica, Facultad de Ingenieria, Universidad de Buenos Aires, Paseo Colon 850, 1063 Buenos Aires, Argentina.

Reprint requests to Prof. Dr. S. Steeb, Max-Planck-Institut für Metallforschung, Institut für Werkstoffwissenschaften, Seestraße, 7000 Stuttgart.

0340-4811 / 83 / 1000-1098 $ 01.3 0/0. – Please order a reprint rather than making your own copy.

Table 1. T = temperature of the melt; ϱ_0 = mean atomic density; Q^{I}, ΔQ^{I} = position and half width of the main peak, respectively; ξ = correlation length; Q^{II}, Q^{III} = position of the second and third maxima of $S(Q)$ (subscripts indicate first and second partial maximum of the second peak).

Substance	T [°C]	ϱ_0 [Atoms/Å^3]	Q^{I} [Å^{-1}]	ΔQ^{I} [Å^{-1}]	$\xi = 2\pi/\Delta Q^{\mathrm{I}}$ [Å]	Q_1^{II} [Å^{-1}]	Q_2^{II} [Å^{-1}]	Q^{III} [Å^{-1}]
$Ni_{81}B_{19}$ melt	1150	0.0860	3.05	0.81	7.76	5.40	6.15	8.25
$Ni_{81}B_{19}$ amorphous	–	0.1020	3.19	0.53	11.86	5.44	6.37	8.01
$Fe_{83}B_{17}$ melt	1200	0.0840	3.03	0.62	10.13	5.23	6.07	8.03
$Fe_{80}B_{20}$ amorphous	–	0.0910	3.12	0.48	13.09	5.21	6.19	7.86
$Ni_{53}B_{47}$ melt	1050	0.0944	3.08	1.30	4.83	5.28	–	–
$Ni_{43}B_{57}$ melt	1450	0.0978	3.07	–	–	5.36	–	7.92

Table 2. Structural parameters. R^{I}, N^{I} = atomic distance and total coordination number, respectively, calculated from the total pair correlation function; $R_1^{\mathrm{II}}/R^{\mathrm{I}}$, $R^{\mathrm{III}}/R^{\mathrm{I}}$ = normalized atomic distances (referred to R^{I}) (the subscripts at R^{II} indicate first and second partial maxima of the second peak, respectively).

Substances	N^{I}	R^{I} [Å]	R_1^{II} [Å]	R_2^{II} [Å]	R^{III} [Å]	$\frac{R_1^{\mathrm{II}}}{R^{\mathrm{I}}}$	$\frac{R_2^{\mathrm{II}}}{R^{\mathrm{I}}}$	$\frac{R^{\mathrm{III}}}{R^{\mathrm{I}}}$
$Ni_{81}B_{19}$ melt	11.9	2.50	4.25	4.72	6.52	1.70	1.89	2.61
$Ni_{81}B_{19}$ amorphous [4]	12.9	2.50	4.10	4.84	6.28	1.64	1.94	2.51
$Fe_{83}B_{17}$ melt [5]	12.6	2.55	4.35	4.79	6.65	1.71	1.88	2.61
$Fe_{80}B_{20}$ amorphous [5]	12.8	2.53	4.15	4.93	6.38	1.64	1.95	2.52
$Ni_{53}B_{47}$ melt	10.0	2.58	4.15	4.83	6.37	1.61	1.87	2.47
$Ni_{43}B_{57}$ melt	8.2	2.57	4.15	5.10	6.30	1.61	1.98	2.45
Model [8]	–	–	–	–	–	1.65	1.93	2.52

The following features of the two Ni-B-curves shall be mentioned: The $S^{\mathrm{AL}}(Q)$-curve of the melt shows smaller amplitudes than that of the amorphous alloy. The main maximum of the melt lies at smaller Q's. The half width ΔQ^{I} is larger for the curve obtained with the melt and therefore according to $\xi = 2\pi/\Delta Q^{\mathrm{I}}$ the correlation length ξ is smaller than in the amorphous state. The corresponding values are listed up in Table 1.

The most remarkable feature is the pronounced asymmetry of the second maximum of the structure factor of the $Ni_{81}B_{19}$-melt. In the case of amorphous alloys this asymmetry normally occurs as shoulder or as subpeak. As shown in [6] and [7], by means of dense random hard sphere packing models, the weakening of the shoulder on the second maximum of the structure factor of the melt can be explained by a smearing out of the tetrahedral atomic arrangement of the amorphous alloy. For melts up to now a similar behaviour was only observed in two cases, namely for the Fe-B-system [5] and for the Mn-Si-system [3]. The behaviour of the Ni-B-melt is in accordance with the hypothesis already presented in [3] according to which melts showing an asymmetry or a splitting up of the second maximum of the total structure factor are glass-formers. For the Fe-B-system one can state that the asymmetry of the second maximum is more pronounced for the melt as well as for the amorphous substance compared to the corresponding specimens from the Ni-B-system.

b) Pair Correlation Function and Coordination Number

From the Ashcroft-Langreth total structure factors $S^{\mathrm{AL}}(Q)$ the corresponding total pair correlation functions $G^{\mathrm{AL}}(R)$ for amorphous and liquid $Ni_{81}B_{19}$-alloys were calculated following [3]. They are plotted in Fig. 2 together with the total pair correlation functions already reported for amorphous $Fe_{80}B_{20}$ [5] and for molten $Fe_{83}B_{17}$ [5]. One recognizes that the pronounced splitting up of the second maximum of the amorphous curve is preserved in the molten

curve as a strong asymmetry just in the same way as for the Fe-B-system. This behaviour of a second maximum in $G^{AL}(R)$ in the molten state up to now only could be observed for melts from the Mn-Si- [3] and the Fe-B-system [5]. One can also see from Fig. 2 that (as was already discussed in a)) the correlation length for the topological short range order is shorter for the nickel-boron melt compared to the amorphous alloy.

The normalized atomic distances for molten and amorphous nickel-boron and iron-boron alloys as well as for a tetrahedral model [8] are listed in Table 2. While the values for both amorphous alloys show a rather good agreement with the data obtained from the model the normalized atomic distances taken from the total pair correlation functions of the melts show certain deviations: Compared to the model R_1^{II}/R^I is shifted to a higher and R_2^{II}/R^I to a lower value. As outlined in a previous study on molten $Fe_{83}B_{17}$ [5] this behaviour is explained by a higher degree of imperfection of the tetrahedral atomic arrangement in the molten state than in the amorphous state (compare [6] and [7]).

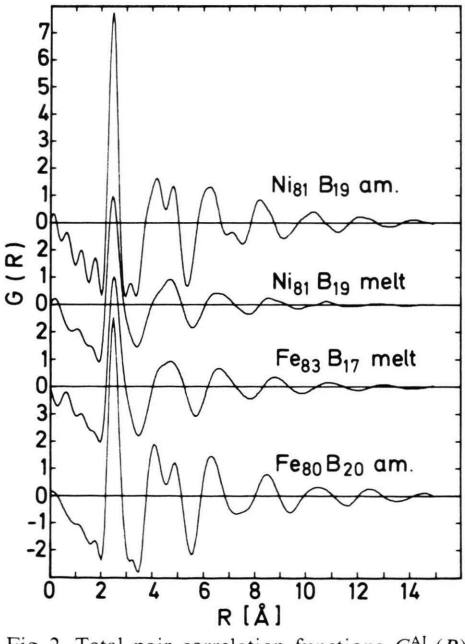

Fig. 2. Total pair correlation functions $G^{AL}(R)$ calculated from the $S^{AL}(Q)$ of Fig. 1 for amorphous $Ni_{81}B_{19}$ [4], molten $Ni_{81}B_{19}$, molten $Fe_{83}B_{17}$ [5], and amorphous $Fe_{80}B_{20}$ [5].

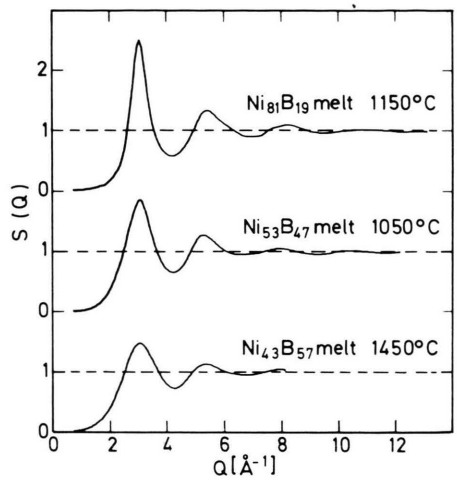

Fig. 3. Total structure factors for the $Ni_{81}B_{19}$, $Ni_{53}B_{47}$, and $Ni_{43}B_{57}$ molten alloys.

We can also see from the values of Table 2 that the first interatomic distance R^I taken from the total pair correlation function is the same for the amorphous and for the molten nickel-boron alloy containing 19 at.% boron. The Ashroft-Langreth total pair correlation function for $Ni_{81}B_{19}$ can be expressed in terms of the partial correlation functions as follows:

$$G^{AL}(R) = 0.804\, G_{NiNi} + 0.001\, G_{BB} + 0.067\, G_{NiB}\,. \quad (1)$$

These weighting factors show that the interatomic distances reported in Table 2 mainly represent Ni-Ni distances. This explains the good coincidence of the position of the main maximum at 2.50 Å and the nickel atomic diameter of 2.48 Å [9].

From the total pair correlation function of the molten nickel-boron alloy with 19 at.% boron, the total coordination number N^I for the first shell was taken and in Table 2 compared with the values of N^I obtained from amorphous $Ni_{81}B_{19}$ [4] and from molten and amorphous iron-boron alloys [5].

II. Molten Ni-B Containing 47 at.% B

a) Structure Factor

In the upper part of Fig. 3 the measured Ashcroft-Langreth total structure factors for the nickel-boron molten alloys containing 19 and 47 at.% boron, respectively, are compared. It can be observed that the $Ni_{53}B_{47}$ alloy which does not belong to the glass

forming composition range of the nickel-boron system shows no indication of a shoulder at the second maximum of the total structure factor. Furthermore, this boron-rich molten alloy presents a remarkable low intensity of the main peak of $S^{AL}(Q)$.

b) Pair Correlation Function and Coordination Number

In Fig. 4 the Ashcroft-Langreth total pair correlation functions $G^{AL}(R)$ are plotted for the nickel-boron molten alloys containing 19 at.% and 47 at.% boron, respectively. It can be seen that the spacial extension of the topological ordering in the $Ni_{53}B_{47}$-melt which does not fall into the glass-forming composition range is substantially shorter than in the $Ni_{81}B_{19}$-melt (compare also the ξ-values in Table 1).

From the $G^{AL}(R)$-curves the interatomic distances R^{I}, R_1^{II}, etc. and their normalized values R_1^{II}/R^{I}, R_2^{II}/R^{I}, etc. were obtained (see Table 2). The main peak of the total pair correlation for the $Ni_{53}B_{47}$-melt is slightly displaced to larger R-values in comparison to the $Ni_{81}B_{19}$ molten alloy. This observation is surprising for the following reason: The $G^{AL}(R)$ pair correlation function for the melt containing 47 at.% boron can be expressed as function of the partial pair correlation functions as follows [3]:

$$G^{AL}(R) = 0.515\, G_{NiNi}(R) + 0.013\, G_{BB}(R) + 0.163\, G_{NiB}(R). \quad (2)$$

One would thus expect, in comparison with the case of $Ni_{81}B_{19}$ (see Eq. (1)), due to the greater influence of the Ni-B distance, which is smaller than the Ni-Ni distance, a displacement of the first maximum of the $G^{AL}(R)$-curve to lower R-values.

As the main peak of the total pair correlation function, however, still represents mainly the Ni-Ni correlation, its observed displacement to larger R-values for the $Ni_{53}B_{47}$-melt means that the boron excess leads in this case to an expansion of the Ni-Ni interatomic distances. The second maximum of the total pair correlation function shows for the boron rich liquid alloy a pronounced splitting up compared with the case of the $Ni_{81}B_{19}$ melt with a lower R-value for the first partial maximum and a higher R-value for the second partial maximum of the second peak, respectively.

The main peak of $G^{AL}(R)$ for the $Ni_{53}B_{47}$-melt shows an asymmetry at its left hand side which was not observed with the $Ni_{81}B_{19}$-melt. The weighting factors in (1) and (2) support the identification of this asymmetry as contribution of the Ni-B correlation. Fitting the main peak of the total pair correlation function obtained with the $Ni_{53}B_{47}$ molten alloy in Fig. 4 by a Gaussian curve in a similar way as reported in [10] yields by forming the difference between the fit and the experimental curve a further coordination shell which is centered at about 2 Å (see Figure 5).

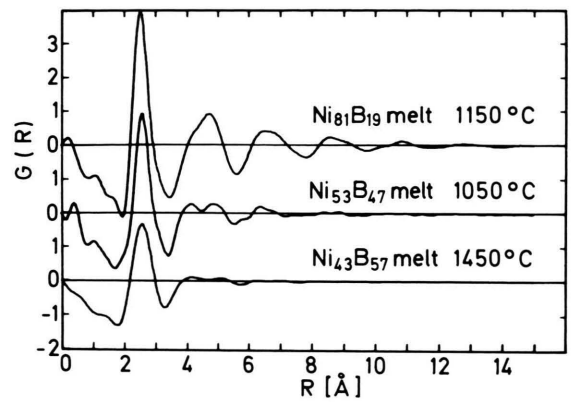

Fig. 4. Total pair correlation functions for the $Ni_{81}B_{19}$, $Ni_{53}B_{47}$, and $Ni_{43}B_{57}$ molten alloys.

III. Molten Ni-B Containing 57 at.% B

a) Structure Factor

Figure 3 also shows the Ashcroft-Langreth total structure factor for the Nickel-Boron molten alloy containing 57 at.% B.

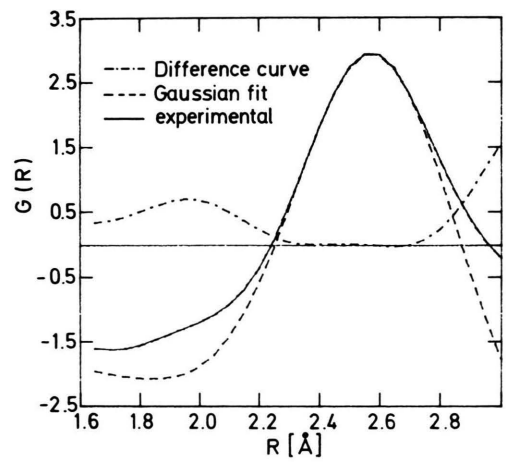

Fig. 5. Molten $Ni_{53}B_{47}$. Pair correlation functions $G(R)$. Fitting of the main maximum by a Gaussian curve.

Compared to the curve obtained with 47 at.% B the following features can be observed:

The specimen with higher Boron-content yields a larger amount of scattered intensity at $\sim 1.5 Å^{-1}$. Furthermore, the first and second maxima have become smaller, and finally also the asymmetry of the second maximum has decreased. Thereby as a measure for the asymmetry the relative difference was used of the gradients of the tangents through the points of inflection on the left hand and on the right hand side of the second maximum.

b) Pair Correlation Function $G(R)$

In Fig. 4 the Ashcroft-Langreth total pair correlation function of the $Ni_{43}B_{57}$ molten alloy is compared with those of the melts containing 19 and 47 at.% boron. The specimen with higher Boron-content yields smaller maxima. Furthermore one observes that the first partial maximum of the second maximum lies at the same R-value as that of $Ni_{53}B_{47}$ whereas the second partial maximum is shifted by 0.3 Å to larger R's.

One can state that with the melts containing 57 at.%, 47 at.%, and 19 at.% B, i.e. that in the direction to the glass forming composition the asymmetry of the second maximum of the structure factor increases. In the region of the second maximum of the corresponding $G(R)$-curves the two partial maxima approach one another thus yielding at last one maximum with a shoulder on the left hand side. Finally it should be mentioned that similar observations also were done regarding the two amorphous alloys $Ni_{64}B_{36}$ and $Ni_{82}B_{18}$ (see [2]).

Acknowledgement

Thanks are due to the Deutsche Forschungsgemeinschaft (DFG), Bad Godesberg, for financial support of this work.

[1] P. Lamparter, W. Sperl, S. Steeb, and J. Blétry, Z. Naturforsch. **37a,** 1223 (1982).
[2] G. S. Chadha, N. Cowlam, H. A. Davies, and I. W. Donald, J. Non Cryst. Solids **44,** 265 (1981).
[3] E. Nassif, P. Lamparter, B. Sedelmeyer, and S. Steeb, Z. Naturforsch. **38a,** 1093 (1983).
[4] W. Sperl, Doctor thesis, University of Stuttgart, 1982.
[5] E. Nold, G. Rainer-Harbach, P. Lamparter, and S. Steeb, Z. Naturforsch. **38a,** 325 (1983).
[6] T. Ichikawa, Phys. Stat. Sol. **29a,** 293 (1975).
[7] J. Blétry, Thèse d'Etat, Grenoble 1979.
[8] S. Takeuchi and S. Kobayashi, Phys. Stat. Sol. **65a,** 315 (1981).
[9] W. Hume Rothery and G. V. Raynor, The Structure of Metals and Alloys, Inst. Metals, London 1954.
[10] E. Nassif, P. Lamparter, W. Sperl, and S. Steeb, Z. Naturforsch. **38a,** 142 (1983).